Journal of Molecular Graphics and Modelling 50 (2014) 113–124

Contents lists available at ScienceDirect

Journal of Molecular Graphics and Modelling

journal homepage: www.elsevier.com/locate/JMGM

Effect of D23N mutation on the dimer conformation of amyloid β-proteins: *Ab initio* molecular simulations in water

Akisumi Okamoto[a], Atsushi Yano[a], Kazuya Nomura[a], Shin'ichi Higai[b], Noriyuki Kurita[a,*]

[a] *Department of Computer Science and Engineering, Toyohashi University of Technology, 1-1 Hibarigaoka, Tempaku-cho, Toyohashi, Aichi 441-8580, Japan*
[b] *Murata Manufacturing Co., Ltd., 1-10-1 Higashikotari, Nagaokakyo, Kyoto 617-8555, Japan*

ARTICLE INFO

Article history:
Accepted 15 March 2014
Available online 16 April 2014

Keywords:
Alzheimer's disease
Amyloid β-protein
Iowa mutation
Aggregation
Specific interaction
Molecular orbital

ABSTRACT

The molecular pathogenesis of Alzheimer's disease (AD) is deeply involved in aggregations of amyloid β-proteins (Aβ) in a diseased brain. The recent experimental studies indicated that the mutation of Asp23 by Asn (D23N) within the coding sequence of Aβ increases the risk for the pathogeny of cerebral amyloid angiopathy and early-onset familial ADs. Fibrils of the D23N mutated Aβs can form both parallel and antiparallel structures, and the parallel one is considered to be associated with the pathogeny. However, the structure and the aggregation mechanism of the mutated Aβ fibrils are not elucidated at atomic and electronic levels. We here investigated solvated structures of the two types of Aβ dimers, each of which is composed of the wild-type or the D23N mutated Aβ, using classical molecular mechanics and *ab initio* fragment molecular orbital (FMO) methods, in order to reveal the effect of the D23N mutation on the structure of Aβ dimer as well as the specific interactions between the Aβ monomers. The results elucidate that the effect of the D23N mutation is significant for the parallel structure of Aβ dimer and that the solvating water molecules around the Aβ dimer have significant contribution to the stability of Aβ dimer.

1. Introduction

Aggregations of amyloid β-proteins (Aβ) have been considered to play a key role in the mechanism of molecular pathogenesis of Alzheimer's disease (AD), which is a serious dementia, accompanied by senile plaques in a diseased brain [1]. The proteolytic cleavage of the amyloid precursor protein (APP) by β- and γ-secretases produces Aβs [2], and the γ-secretase cleave APP at its several alternative sites to produces Aβs of varied lengths. The most abundant Aβs contained in the senile plaques are Aβ40 and Aβ42 [2,3], each of which has 40 or 42 amino acid residues, respectively. Aβ42 was found to aggregate more rapidly and comprise a major component of the senile plaques in a diseased brain [4–6]. These plaques cause a death of neuronal cells in a diseased brain [7]. Since Aβ peptides have several hydrophobic amino acid residues, Aβs form strong aggregates in water due to the hydrophobic interactions between these residues, leading to a fibril formation of Aβs [8]. Accordingly, it is expected that compounds having a strong binding affinity to Aβ can inhibit the Aβ aggregation and be a potent inhibitor for the amyloidogenesis and pathogenesis of AD.

With respect to the fibril structure of the wild-type Aβs, numerous structural studies [9–20] based on solid-state nuclear magnetic resonance (SSNMR) or electron paramagnetic resonance (EPR) measurement have revealed that the most of the fibrils are stabilized in a common conformation with parallel β-sheets. In contrast, the recent SSNMR measurements on polymorphic samples of fibrils formed by the Asp23-to-Asn (D23N), or Iowa mutant of Aβ (D23N-Aβ) have revealed that a large fraction of the D23N-Aβ fibrils contain antiparallel β-sheets [21,22]. The D23N mutation causes a familial, early-onset neurodegeneration involving extensive cerebral amyloid angiopathy [23]. It is thus likely that the antiparallel β-sheets of the D23N-Aβ fibrils exert distinct pathogenic effects.

The experimental studies [21,24] based on electron microscopy, X-ray diffraction and SSNMR spectroscopy have revealed that the D23N-Aβ40 forms fibrils considerably faster than the wild-type Aβ40 (WT-Aβ40) without a lag phase. In addition, SSNMR measurements indicate that only a minority of the D23N-Aβ40 fibrils contains the parallel β-sheet structure commonly found in the WT-Aβ40 fibrils, while the majority of the D23N-Aβ40 fibrils have the antiparallel β-sheet structures. These antiparallel structures were found to be thermodynamically metastable with respect to conversion to the parallel structure under typical conditions [22]. However, it is not elucidated yet why only the D23N-Aβ40 fibril forms the antiparallel β-sheet structure.

* Corresponding author. Tel.: +81 532 44 6875; fax: +81 532 44 6875.
E-mail address: kurita@cs.tut.ac.jp (N. Kurita).

http://dx.doi.org/10.1016/j.jmgm.2014.03.004
1093-3263/

In addition, the reason why the WT-Aβ40 fibrils have only the parallel β-sheet structure is not clarified yet. In the SSNMR analysis for the WT-Aβ40 fibrils [22], it is predicted that the electrostatic interaction between Asp23 of a certain Aβ and Lys28 of the neighboring Aβ can stabilize a parallel conformations of fibrils (PDB ID: 2BEG [25] and 2LMN [26]). In contrast, in the antiparallel conformation, since Asp23 and Lys28 are separated at least 9.6 Å in the direction of the fibril axis, the attractive interaction between these residues is weak. As a result, the antiparallel conformation of the WT-Aβ fibril is less stable than the parallel conformation. By introducing the D23N mutation into Aβ40, the charged residue Asp is replace by the noncharged residue Asn, so that the electrostatic attractive interactions between Aβ40 monomers in the parallel conformation fibril are weakened. As a result, the stability of the parallel conformation is expected to become similar to that of the antiparallel conformation [22]. Consequently, it can be possible for the antiparallel conformation of D23N-Aβ40 fibril to appear as a metastable conformation.

In order to elucidate the effect of the D23N mutation on the Aβ dimer conformations at atomic and electronic levels, we here investigated stable structures for the solvated dimers composed of the wild-type or the D23N mutated Aβ, by use of classical molecular mechanics (MM) and *ab initio* fragment molecular orbital (FMO) [27–35] simulations. In addition, based on the electronic properties of the dimers evaluated by the FMO calculations, we highlighted the residues of Aβ contributing mainly to the dimer formation and elucidated the effect of the D23N mutation on the specific interactions between Aβ monomers. The results are useful for predicting the difference in the initial stage of Aβ aggregations between the WT-Aβ and the D23N-Aβ.

2. Details of molecular simulations

2.1. Optimization of Aβ dimer structures in water

As the initial structures of Aβ dimers with a parallel or an antiparallel conformation, we here employed the PDB structures of the parallel Aβ fibrils (PDB ID: 2LMN) [26] and the antiparallel Aβ fibrils (PDB ID: 2LNQ) [22], respectively. The PDB structure with the parallel conformation [26] has two hexamers of WT-Aβs, and we adopted the two centrally-located C and D chains of the first hexamer as the initial structure of the parallel WT-Aβ dimer. On the other hand, the PDB structure with the antiparallel structure [22] is for the octamer of D23N-Aβs, and its D and E chains located around the center of the fibril were adopted as the initial structure for the antiparallel D23N-Aβ dimer. In the PDB structure for the parallel WT-Aβ fibril [26], the positions of the 1–8 residues of Aβ are missing, while the 1–14 residues are missing in the antiparallel PDB structure [22]. To conform in size between the two structures, we cut out the 9–14 residues of the parallel structure to produce the parallel WT-Aβ(15–40) dimer, because the 1–14 residues are likely to be partially or fully disordered [13–15,22,25,26]. Finally, the N- and C-terminals of Aβ are terminated by the acetyl and the NH_2, respectively.

In addition, by use of SWISS-MODEL [36], the Asp23 residues in the parallel WT-Aβ(15–40) dimer were mutated by Asn to produce the initial structure for the parallel D23N-Aβ(15–40) dimer, while the Asn23 residues in the antiparallel D23N-Aβ(15–40) dimer were mutated by Asp to produce the antiparallel WT-Aβ(15–40). In this paper, we refer the parallel and the antiparallel WT-Aβ(15–40) dimers, and the parallel and the antiparallel D23N-Aβ(15–40) dimers as parallel WT-Aβ, antiparallel WT-Aβ, parallel D23N-Aβ and antiparallel D23N-Aβ dimers, respectively.

These four types of Aβ(15–40) dimers were solvated in a water box of the size of the twice of the Aβ dimer. In fact, the number of solvating water molecules for each dimer is 6271 (parallel WT-Aβ), 6322 (antiparallel WT-Aβ), 6309 (parallel D23N-Aβ) and 6247 (antiparallel D23N-Aβ), respectively. The solvated structures were fully optimized by the classical MM method implemented in the molecular simulation program package GROMACS Ver.4.5.3 [37]. In the MM optimizations, we used the FF99SB force field [38] in combinations with the TIP4P-Ew water model [39], because the previous replica exchange molecular dynamics (MD) calculations [40] shown that this combination of the force field and the water model produces an ensemble of configurations for solvated Aβ(21–30), being in good agreement with the NMR data. The threshold value of the energy-gradient for the convergence of the MM optimization was set to 0.0001 kcal/mol/Å.

2.2. Ab initio FMO calculations for Aβ dimers in water

The electronic properties for the solvated Aβ dimers were investigated by the *ab initio* FMO method [27–35], to elucidate which amino acid residues in Aβ are important for the stability of the solvated Aβ dimers. In the FMO calculation, the target molecule is divided into units called “fragment”, and the electronic properties of the target molecule are estimated from the electronic properties of the monomers and the dimers of the fragments. The specific interactions between the fragments can be investigated from the interaction energies obtained by the FMO calculation.

In the present FMO calculations, we investigated the relative stability between the parallel and the antiparallel conformations for the Aβ(15–40) dimer, with the solvating water molecules considered explicitly. We chose the 765 water molecules solvating nearest to the Aβ(15–40) dimer in the MM-optimized structure of the solvated dimer. These water molecules exist within a 6 Å distance from the surface of the dimer. The C- and N-terminals of Aβ(15–40) were terminated by the acetyl and the NH_2 groups, respectively. These groups were considered as the 14th and the 41st residues of Aβ(15–40) in the FMO calculations. Each residue of Aβ(15–40) and each water molecule were assigned as a fragment, because this fragmentation enables us to evaluate the interaction energies between the Aβ residues and between the residue and the solvating water molecules. Total number of the fragments for the solvated Aβ(15–40) dimer is 821, and total charge is assigned 0 and +2 for the WT-Aβ dimer and the D23N-Aβ dimer, respectively.

The *ab initio* MP2/6-31G method was employed to investigate accurately the π–π stacking, NH–π and CH–π interactions between the residues of Aβ(15–40). We used the FMO calculation program ABINIT-MP Ver.6.0 [41]. By considering water molecules explicitly, we attempted to elucidate the influence of solvating water molecules on the stabilization of the dimer conformation. In addition, to elucidate which amino acid residues of Aβ(15–40) contribute to the stability of the dimer conformation, we investigated the specific interactions between the fragments by the FMO method at an electronic level. It is noted that the interaction energies between the charged amino acid residues are overestimated, because the FMO calculations are preformed in vacuum with solvating water molecules considered explicitly.

3. Results and discussion

3.1. Optimized structures of solvated Aβ dimers

As shown in Fig. 1a, in the solvated structure of the parallel WT-Aβ(15–40) dimer, Asp23 of monomer-A and Lys28 of monomer-B form a salt-bridge between the monomers. The previous SSNMR analysis for the WT-Aβ40 fibrils and the MD simulations for the WT-Aβ39 dimer [14,26,42–44] indicated that Glu22/Asp23 and Lys28 form a salt-bridge both in a monomer and between

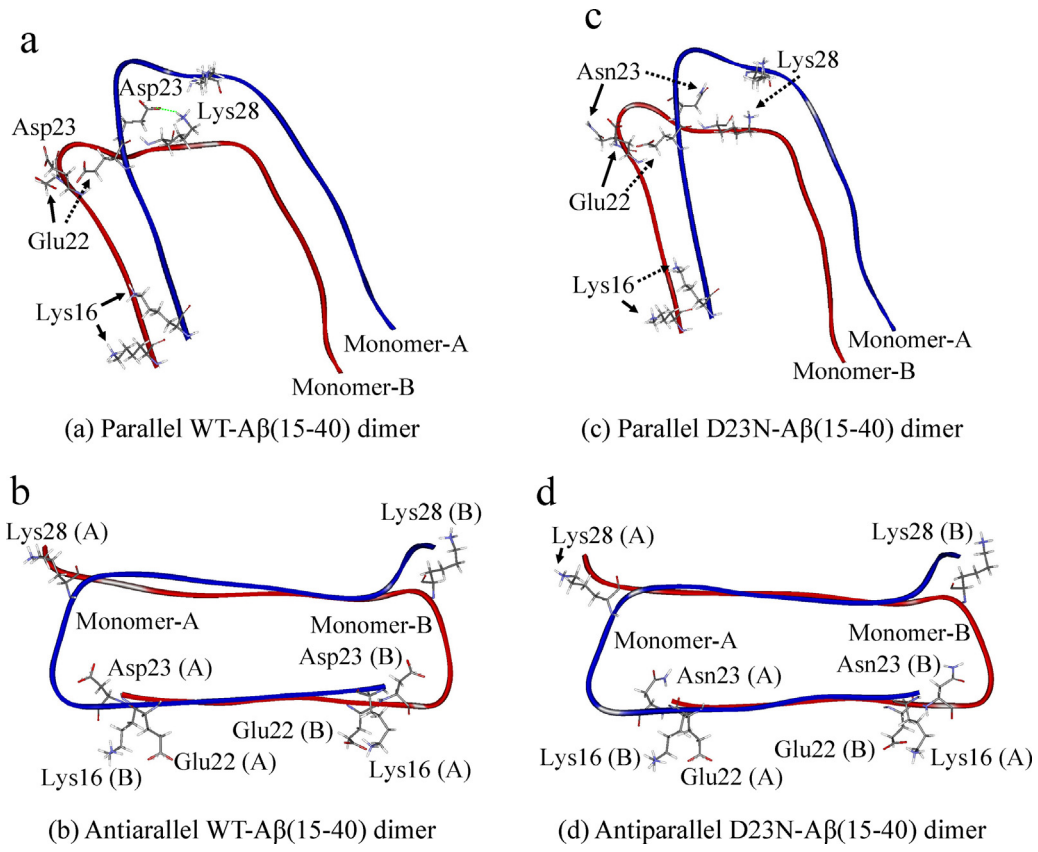

Fig. 1. Structures of the solvated dimers of the WT and the D23N-mutated Aβ(15–40) with a parallel or an antiparallel conformation optimized by classical MM method. Monomer-A is in blue, while Monomer-B is in red. The charged amino acid residues of Aβ(15–40) are displayed in a stick model. A green dot-line indicates a salt bridge between Asp23 of Monomer-A and Lys28 of Monomer-B.

monomers. In addition, it was predicted that the formation of the salt-bridge is a driving force for the oligomerization and the fibrillation of Aβs [25,26,44]. Our present results of the structure optimizations in water by the classical MM method elucidate that the salt-bridge between Asp23 and Lys28 is formed only between the monomers in the parallel WT-Aβ dimer, while there is no salt-bridge in the WT-Aβ monomer.

On the other hand, in the antiparallel WT-Aβ(15–40) dimer shown in Fig. 1b, Glu22/Asp23 of monomer-A and Lys28 of monomer-B are significantly separated from each other, and there is no salt-bridge between the monomers. As for the intramonomer salt-bridge, since the side chain of Lys28 is exposed to solvent outside of the core, Lys28 cannot form a salt-bridge with Glu22/Asp23 of the same monomer. The previous experiment [22] suggested a possibility for an electrostatic interaction between the Lys28 side chain and the COO^- group of the C-terminal of Val40 in the other Aβ monomer. However, in our present study, since the C-terminal of Aβ is terminated by the noncharged acetyl group, the electrostatic interaction is not observed. Consequently, the present MM-optimization in water indicates that there is almost no possibility for the salt-bridge between Glu22/Asp23 and Lys28 both within a monomer and between monomers in the antiparallel WT-Aβ(15–40) dimer.

To elucidate the effect of the D23N mutation on the structure of Aβ(15–40) dimer, we optimized the structures of the parallel and the antiparallel D23N-Aβ dimers in water. As shown in Fig. 1c, in the parallel conformation, the salt-bridge between Asp23 and Lys28 is disappeared by the mutation from Asp23 to noncharged Asn23. As a result, the Lys28 side chain becomes flexible to be exposed to solvent. In the parallel D23N-Aβ dimer, there is a possibility for the salt-bridge between the negatively charged Glu22 and Lys28. However, as shown in Fig. 1c, since the Lys28 side chain is exposed outside the core, the salt-bridge between Lys28 and Glu22 cannot be formed in the parallel D23N-Aβ dimer. The similar results were observed by the previous experiments [21] for the D23N-Aβ40 fibrils. Therefore, the solvated structures of the Aβ dimers obtained by the present molecular simulations seem to be realistic.

The relative positions of Asp23/Asn23 and Lys28 in the antiparallel WT-Aβ(15–40) dimer is hardly affected by the D23N mutation, as shown in Fig. 1b and d. This result may come from the fact that the electrostatic interaction between Asp23 and Lys28 in the antiparallel WT-Aβ dimer is originally weak, so that the D23N mutation has little effect on the electrostatic interaction. As described above, the present molecular simulations elucidate that the effect of the D23N mutation on the structure of the Aβ(15–40) dimer is remarkable for the parallel conformation, while that is little for the antiparallel conformation.

In order to reveal the relative stability between the parallel and the antiparallel conformations for the WT-Aβ(15–40) and the D23N-Aβ(15–40) dimers, we investigated accurately the total energies of the solvated Aβ dimers by use of the *ab initio* MP2/6-31G method of ABINIT-MP Ver.6.0 program [41]. It is noted that the solvating water molecules are indispensable for describing the realistic state of the Aβ dimers in a cell. Table 1 lists the total energies (TEs) of the solvated Aβ dimers, the dimers in vacuum, and the solvating water molecules. To elucidate the effect of solvation, we evaluated the hydration energy (HE) from the following equation.

$$HE = -TE(\text{Solvated A}\beta\text{ dimer}) + TE(\text{A}\beta\text{ dimer}) + TE(\text{Solvating water molecules}).$$

Table 1
Total energies (TE) (kcal/mol) evaluated by the *ab initio* FMO method for the solvated dimers of the wild type (WT) and the D23N-mutated Aβ(15–40), the same dimers in vacuum and the solvating water molecules around the dimer. The hydration energies (HE) for the Aβ(15–40) dimers are estimated as HE = −TE (solvated dimer) + TE (dimer in vacuum) + TE (Solvating water molecules). ΔTE is TE relative to the most stable one, and ΔHE is HE relative to the most stable one.

Structure	Solvated dimer		Dimer in vacuum		Water molecules		HE (kcal/mol)	AHE (kcal/mol)
	TE	ATE	TE	ATE	TE	ATE		
WT parallel	−48371982.0	0.0	−11822891.3	173.1	−36546593.3	194.2	2497.5	519.7
WT antiparallel	−48371829.7	152.4	−11823064.4	0.0	−36546787.5	0.0	1977.8	0.0
d23n parallel	−48347749.0	0.0	−11798611.3	154.3	−36546869.2	0.0	2268.5	316.7
D23N antiparallel	−48347571.2	177.9	−11798765.5	0.0	−36546853.8	15.4	1951.8	0.0

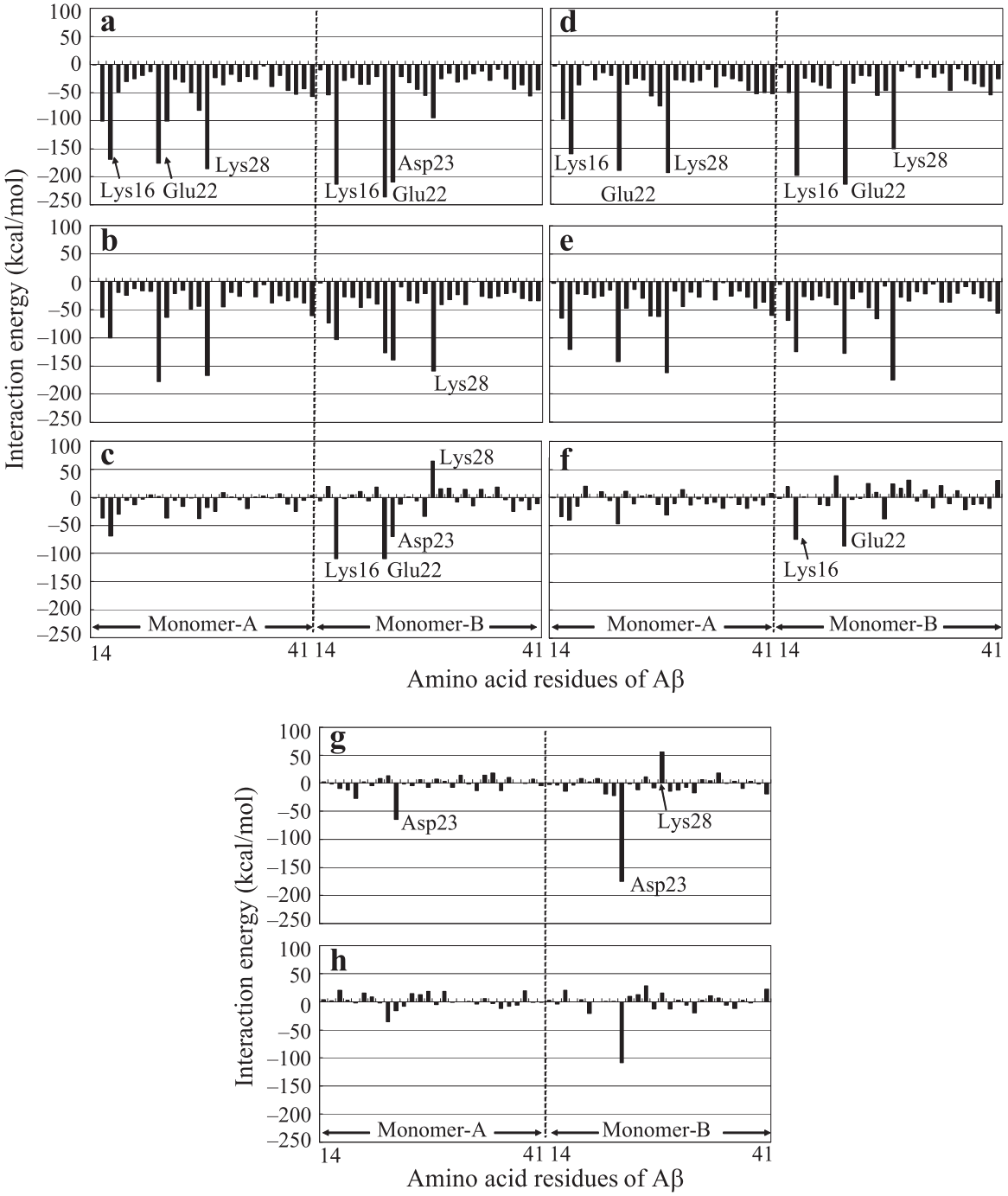

Fig. 2. Interaction energies (IE) between each amino acid residue of Aβ(15–40) and all solvating water molecules: (a) parallel WT-Aβ dimer, (b) antiparallel WT-Aβ dimer, (c) difference in IE between the parallel and the antiparallel WT-Aβ dimers, (d) parallel D23N-Aβ dimer, (e) antiparallel D23N-Aβ dimer, (f) difference in IE between the parallel and the antiparallel D23N-Aβ dimers, (g) difference in IE between the parallel WT-Aβ dimer and the parallel D23N-Aβ dimer, and (h) difference in IE between the antiparallel WT-Aβ dimer and antiparallel D23N-Aβ dimer.

Table 2
Interaction energies (IE) (kcal/mol) evaluated by the *ab initio* FMO method between each solvating water molecule (W1, W2, and so on) and Lys16/Glu22 of Monomer-B in the WT and the D23N-mutated Aβ(15–40) dimers with a parallel (P) or an antiparallel (A) conformation.

	WT-P	WT-A	D23N-P	D23N-A	WT-P	WT-A	D23N-P	D23N-A
W1	−23.4	−36.7	−25.1	−22.2	−23.3	−23.0	−23.7	−24.8
W2	−23.1	−16.9	−22.5	−17.4	−19.3	−22.5	−21.6	−23.7
W3	−22.6	−16.4	−21.0	−15.6	−19.0	−20.7	−21.6	−17.7
W4	−20.4	−16.3	−20.8	−15.2	−18.4	−20.3	−19.9	−17.4
W5	−20.3	−10.2	−11.8	−10.7	−16.8	−15.3	−17.7	−17.1
W6	−13.2	−9.2	−10.6	−8.3	−14.0	−10.3	−17.5	−14.7
W7	−8.8	−7.1	−10.4	−5.5	−10.7	−7.9	−15.0	−10.7
W8	−8.2	−5.3	−9.6	−5.3	−9.8	−7.1	−8.2	−9.2
W9	−7.4	−5.1	−6.0	−4.8	−9.6	−6.3	−7.3	−8.6
W10	−5.7	−4.9	−5.7	−4.8	−8.8	−5.6	−7.1	−6.8
W11	−5.5	−4.7	−5.6	−4.3	−7.7	−5.6	−6.9	−4.9
W12	−5.0	−4.5	−5.5	−4.2	−6.4	−3.8	−6.5	−4.8
W13	−4.1	−3.9	−5.1	−4.0	−5.4	−3.4	−6.3	−3.8
W14	−4.0	−2.8	−5.0	−3.8	−5.2	−3.4	−5.6	−3.4
W15	−3.8	−2.6	−4.7	−3.7	−4.8	−3.3	−5.6	−3.3
W16	−3.4	−2.4	−4.2	−2.9	−4.5	−3.3	−5.4	−3.0
W17	−3.2	−2.3	−4.0	−2.7	−4.2	−3.1	−3.9	−2.6
W18	−2.9	−2.2	−3.4	−2.5	−4.1	−3.0	−3.8	−2.6
W19	−2.9	−1.9	−3.2	−2.4	−3.0	−2.9	−3.7	−2.6
W20	−2.9	−1.9	−3.0	−2.4	−2.9	−2.6	−3.0	−2.5
Total	−190.8	−157.3	−187.1	-142.7	−197.6	−173.3	−210.3	−184.0
Difference		−33.5		−44.4		−24.3		−26.2

Table 1 indicates that the parallel conformation of the solvated Aβ dimer is more stable than the antiparallel one for both the WT- and the D23N-Aβ(15–40) dimers in water. In contrast, the relative stability for the same Aβ dimers in the absence of water molecules is inverse to that for the solvated dimers, indicating that the solvating water molecules affect remarkably on the relative stability between the parallel and the antiparallel conformations of the Aβ dimers. For both the dimers, HE for the parallel conformation is significantly larger than that for the antiparallel conformation. In particular, for the WT-Aβ(15–40) dimer, there is about 520 kcal/mol difference in HE between the parallel and the antiparallel conformations. This large difference is reduced to about 320 kcal/mol by the D23N mutation to Aβ. To elucidate the reason why the parallel conformation has larger hydration energy, we evaluated the surface accessible to solvent. The values are 52.9 (WT parallel), 50.1 (WT antiparallel), 52.5 (D23N parallel) and 50.3 nm^2 (D23N antiparallel), respectively. These values and the hydration energies listed in Table 1 are well correlated with each other, indicating that the parallel conformation has larger accessible surface and is more significantly stabilized by solvation.

In the previous experiments [22] for the D23N-Aβ40 fibrils, the parallel structures were found to be more stable than the antiparallel ones. Therefore, the results listed in Table 1 obtained by our present molecular simulations are confirmed to be qualitatively consistent with the experimental results [22]. Moreover, Table 1 indicates that the hydration energy mostly determines the relative stability between the solvated conformations of the Aβ dimers. It can be explained that the solvating water molecules stabilize the parallel conformation more significantly than the antiparallel one for the Aβ dimers. In the absence of water molecules, the antiparallel conformation is more stable than the parallel one, indicating the possibility that the antiparallel conformation can exist at the early stage of solvation, although only the parallel conformation exist at the fully solvated state. Therefore, the present FMO calculations elucidated that it is important to take proper account of the solvation level around the Aβ dimer for investigating the relative stability between the parallel and the antiparallel conformations of the Aβ dimer in water.

To elucidate the reason for the large difference in HE listed in Table 1, we investigated the interaction energies (IE) [45] between each residue of Aβ(15–40) dimer and the solvating water molecules for the WT- and the D23N-Aβ dimers. As shown in Fig. 2a, b, d and e, the charged residues Lys16, Glu22, Asp23 and Lys28 have strong attractive interactions with the solvating water molecules.

For the WT-Aβ(15–40) dimer, the difference in IE between the parallel and the antiparallel conformations was investigated. As shown in Fig. 2c, the IEs between the water molecules and the charged residues (Lys16, Glu22, Asp23 and Lys28) of the monomer-B are remarkably affected by the change in conformation. As indicated in Fig. 1a, the side chain of Asp23 of the monomer-B in the parallel WT-Aβ dimer is exposed to solvent, resulting in the strong attractive interaction between the Asp23 and the solvating water molecules. On the other hand, in the antiparallel WT-Aβ(15–40) dimer (Fig. 1b), since the side chain of Asp23 of the monomer-B directs to the core region, Asp23 has weak

Table 3
Total energies of solvated Aβ(15–40) dimers and their component structures, and binding energies (BEs) between monomers estimated from these total energies evaluated by the *ab initio* FMO method. BE is estimated as BE = −TE (solvated dimer) + TE (solvated monomer-A) + TE (solvated monomer-B) − TE (solvating water molecules). The results for the dimers of the wild type (WT) and the D23N-mutated Aβ(15–40) with a parallel or an antiparallel conformation are listed.

Structure	Total energy (kcal/mol)				Binding energy (kcal/mol)
	Solvated dimer	Monomer-A	Monomer-B	Water molecules	
WT parallel	−48371982.0	−42459234.2	−42459193.4	−36546593.3	147.8
WT antiparallel	−48371829.7	−42459135.8	−42459208.1	−36546787.5	273.2
D23N parallel	−48347749.0	−42447326.8	−42447185.9	−36546869.2	105.5
D23N antiparallel	−48347571.2	−42447111.7	−42447083.2	−36546853.8	230.1

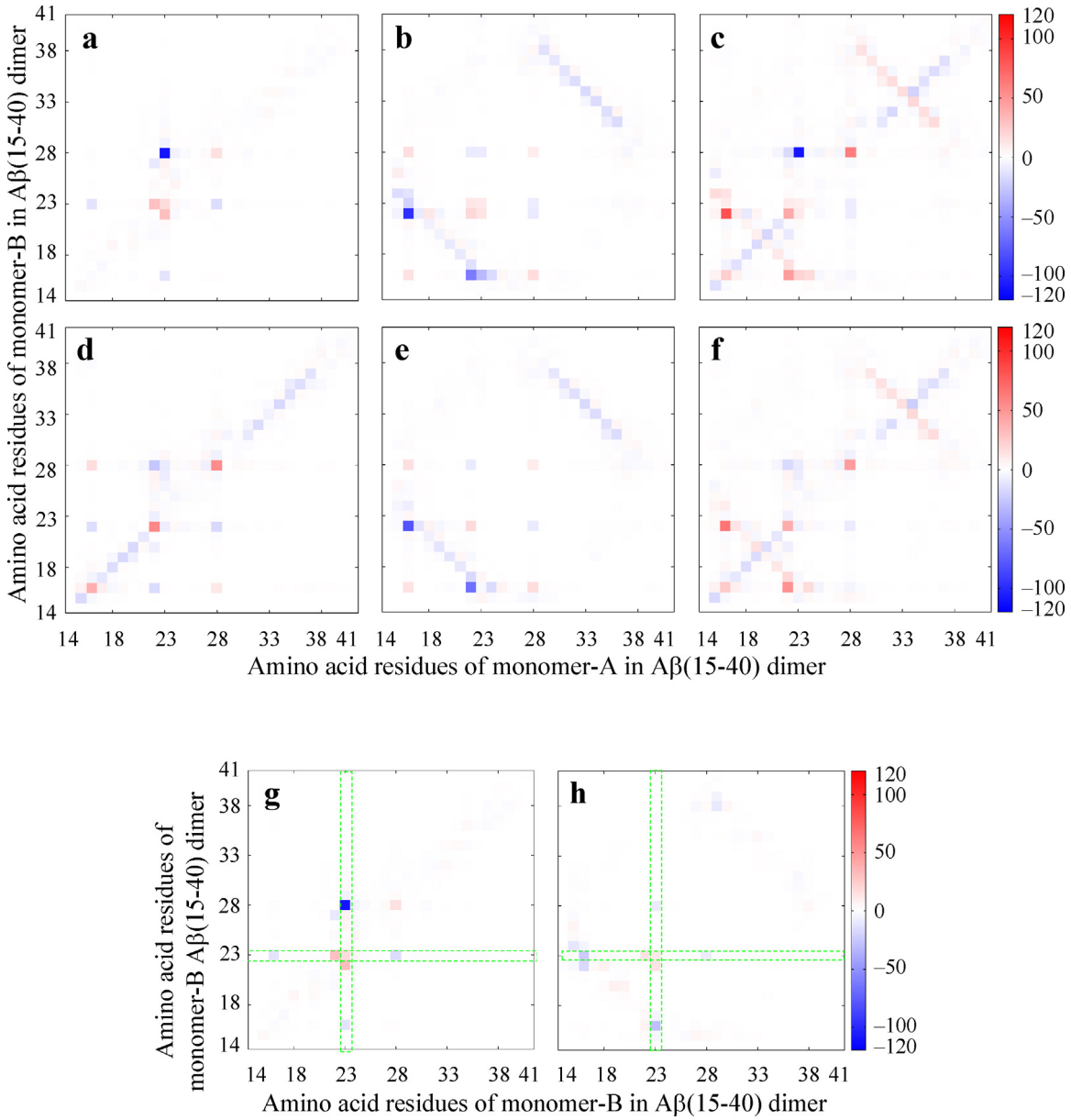

Fig. 3. Interaction energies (IE) between each amino acid residue of Monomer-A and B of Aβ(15–40) dimer: (a) parallel WT-Aβ dimer, (b) antiparallel WT-Aβ dimer, (c) difference in IE between the parallel and the antiparallel WT-Aβ dimers, (d) parallel D23N-Aβ dimer, (e) antiparallel D23N-Aβ dimer, (f) difference in IE between the parallel and the antiparallel D23N-Aβ dimers, (g) difference in IE between the parallel WT-Aβ dimer and the parallel D23N-Aβ dimer, and (h) difference in IE between the antiparallel WT-Aβ dimer and the antiparallel D23N-Aβ dimer.

attractive interactions with the water molecules. As for the Lys28 in the parallel conformation (Fig. 1a), Lys28 of the monomer-B and Asp23 of the monomer-A form a salt-bridge, so that the Lys28 side chain directs to the inner core and cannot interact with the solvating water molecules significantly. On the other hand, in the antiparallel WT-Aβ(15–40) dimer (Fig. 1b), both the Lys28 residues direct to the outside of the core and have strong attractive interactions with the solvating water molecules. As for the Lys16 and Glu22 residues in the antiparallel WT-Aβ(15–40) dimer, both the residues exist near to each other and the charges of the two residues are canceled out. As a result, the water molecules cannot hydrated strongly around the residues. In order to confirm such electronic states, the IEs between Lys16/Glu22 and each water molecule were investigated by the FMO method. Table 2 lists the IEs in the decreasing order of the magnitude of the attractive interaction for the 20 water molecules for each complex. The total energies listed in the last line of Table 2 indicate that the interaction between Lys16/Glu22 and water molecules is stronger in the parallel conformation than in the antiparallel one. This result can be explained by the Lys16-Glu22 pair formed in the antiparallel conformation, as shown in Fig. 1b. As a result, the positive charge of Lys16 and the negative charge of Glu22 are canceled out. Therefore, water molecules cannot hydrate around these residues. On the other hand, in the parallel WT-Aβ(15–40) dimer, Lys16 and Glu22 are separated from each other and their side chains are exposed to solvent, resulting in the strong attractive interaction between Lys16/Glu22 and the solvating water molecules.

We furthermore investigated the effect of the D23N mutation on the specific interactions between the Aβ residues and the solvating water molecules by *ab initio* FMO method. Fig. 2d and e

shows the interaction energies between each Aβ residue and all solvating water molecules. By the D23N mutation, the charged Asp23 residue is replaced by the noncharged Asn one. As a result, the strong attractive interactions between Asp23 and the water molecules disappear. In particular, the effect is remarkable on the monomer-B of Aβ dimer with the parallel conformation. In addition, since the salt-bridge between Asp23 and Lys28 in the WT-Aβ dimer is vanished away by the D23N mutation, the Lys28 side chain of the monomer-B is exposed to solvent. As a result, the interaction between the Lys28 and water molecules in the parallel conformation is enhanced by the D23N mutation. Therefore it is elucidated that the effect of the D23N mutation appears on the Lys28 of the monomer-B as well as the mutated part in the Aβ dimer with the parallel conformation. In contrast, for the Aβ dimer with the antiparallel conformation, the effect of the D23N mutation is rather small compared with that for the parallel conformation.

3.2. Specific interactions between Aβ monomers in the solvated Aβ dimers

To elucidate the change in binding affinity between Aβ monomers induced by the D23N mutation, we first investigated the binding energy (BE) between monomers in the WT- and the D23N-Aβ(15–40) dimers with a parallel or an antiparallel conformation. BE is evaluated from the total energies (TEs) as BE = −TE (solvated dimer) + TE (solvated monomer-A) + TE (solvated monomer-B) − TE (solvating water molecules). As listed in Table 3, the BEs evaluated by the FMO method for the WT-Aβ(15–40) dimer are 147.8 (parallel conformation) and 273.2 kcal/mol (antiparallel conformation), while those for the D23N-Aβ(15–40) dimer are 105.5 (parallel) and 230.1 kcal/mol (antiparallel), indicating that the two Aβ(15–40) monomers interact more strongly with each other in the antiparallel conformation shown in Fig. 1b and d. This result is consistent with the total energies of the Aβ(15–40) dimers in vacuum listed in

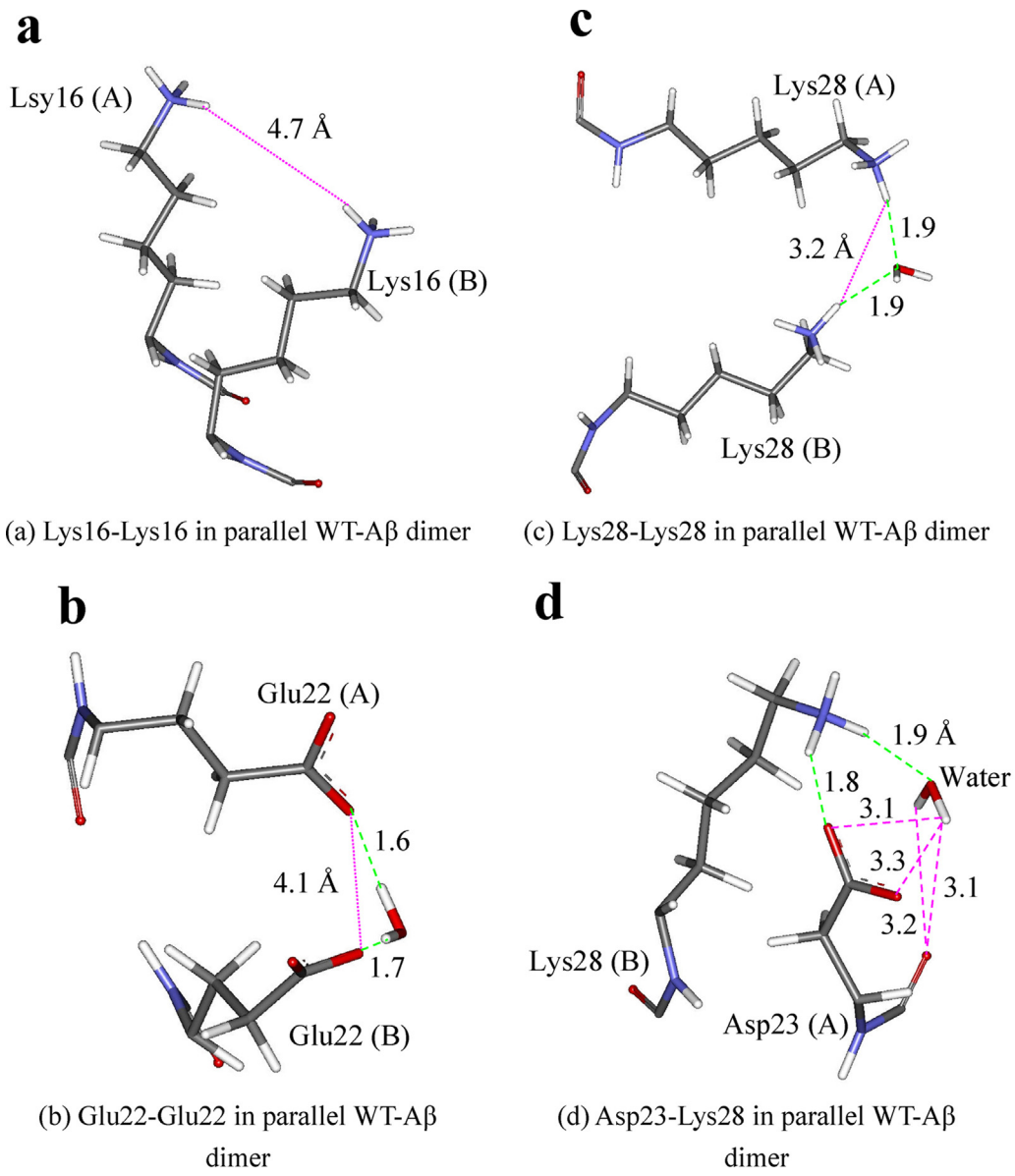

(a) Lys16-Lys16 in parallel WT-Aβ dimer

(c) Lys28-Lys28 in parallel WT-Aβ dimer

(b) Glu22-Glu22 in parallel WT-Aβ dimer

(d) Asp23-Lys28 in parallel WT-Aβ dimer

Fig. 4. Interacting structures between some amino acid residues of Monomer-A and B in the WT- and the D23N-Aβ(15–40) dimers with a parallel conformation; (a) and (e) between Lys16 and Lys16, (b) and (f) between Glu22 and Glu22, (c) and (g) between Lys28 and Lys28, (d) between Asp23-Lys28, (h) between Asn23-Lys28. Green dash-lines indicate hydrogen bonds, while pink dot-lines indicate electrostatic repulsive interactions between charged amino acid residues of Aβ(15–40). Pink dash-lines indicate electrostatic attractive interactions between Asp23 and the solvating water molecules. (For interpretation of the references to color in figure legend, the reader is referred to the web version of the article.)

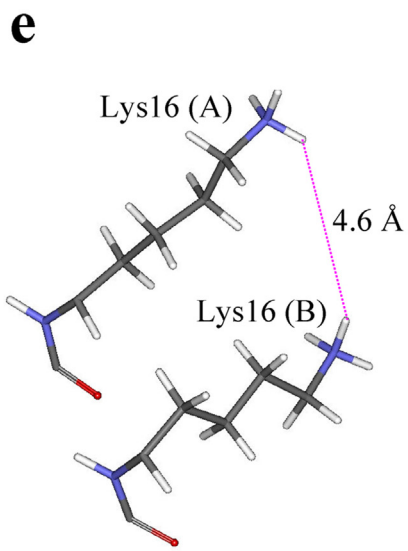

(e) Lys16-Lys16 in parallel D23N-Aβ dimer

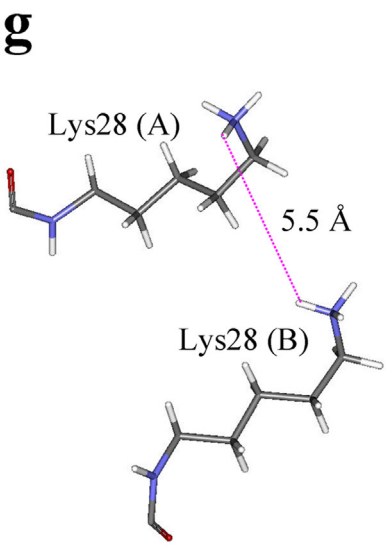

(g) Lys28-Lys28 in parallel D23N-Aβ dimer

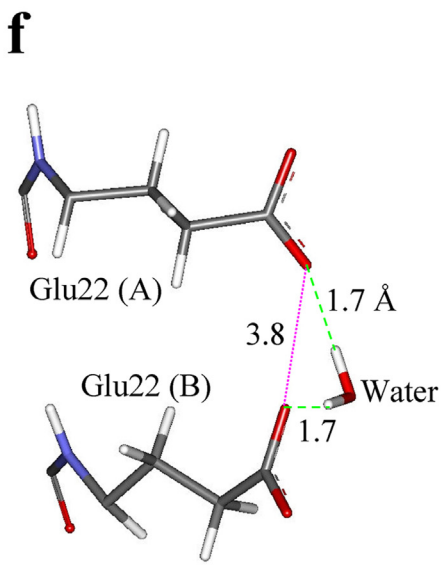

(f) Glu22-Glu22 in parallel D23N-Aβ dimer

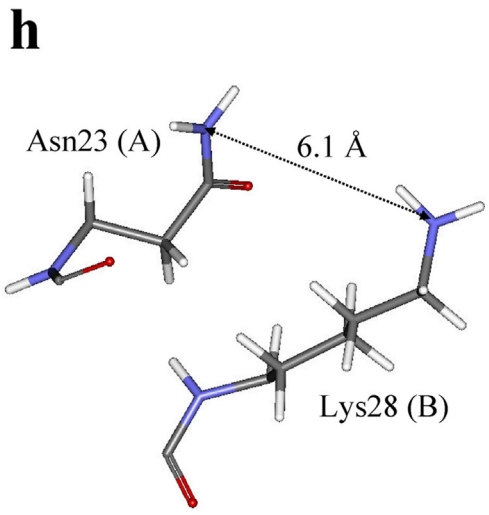

(h) Asn23-Lys28 in parallel D23N-Aβ dimer

Fig. 4. (*continued.*)

Table 1, indicating that the antiparallel conformation is more stable in vacuum. Table 1 also indicates that the Aβ(15–40) dimers in the parallel conformation have larger hydration energy. It is thus likely that water molecules can more easily hydrated around the Aβ(15–40) dimers having the parallel conformation, and that these water molecules can inhibit the aggregation of the Aβ(15–40) dimers. On the other hand, in the antiparallel conformation, the interaction between the Aβ(15–40) dimer and the solvating water molecules is not so strong as in the parallel conformation. Accordingly, it is expected that the Aβ(15–40) dimers with the antiparallel conformation can aggregate easily to form the seed for the Aβ fibril.

In order to elucidate the specific interactions between the Aβ monomers depending on the dimer conformations, we investigated the IE between the amino acid residues of Aβ monomer by the *ab initio* FMO method. The result for the parallel WT-Aβ(15–40) dimer shown in Fig. 3a indicates the strong repulsive interactions for the Lys16–Lys16, Glu22–Glu22 and Lys28–Lys28 pairs. As indicated in Fig. 1a, these charged residues exist close to each other to interact strongly. To clarify the reason for these unique structures, we examined closely the structures of these interacting residues. As shown in Fig. 4a–c, the shortest distance between the residues is 4.7 (Lys16–Lys16), 4.1 (Glu22–Glu22) and 3.2 Å (Lys28–Lys28), respectively. In addition, Fig. 4b and c elucidate a unique water molecule bridging between the Glu22 or the Lys28 residues in the parallel conformation of the WT-Aβ(15–40) dimer.

In addition, the IE map shown in Fig. 3a highlights a strong attractive interaction between Asp23 of monomer-A and Lys28 of monomer-B. As shown in Fig. 4d, the side chains of Asp23 and Lys28 form a salt bridge, and additionally a water molecule bridges between these side chains, resulting in a strong attractive interaction (−119.3 kcal/mol) between Asp23 and Lys28. It is thus

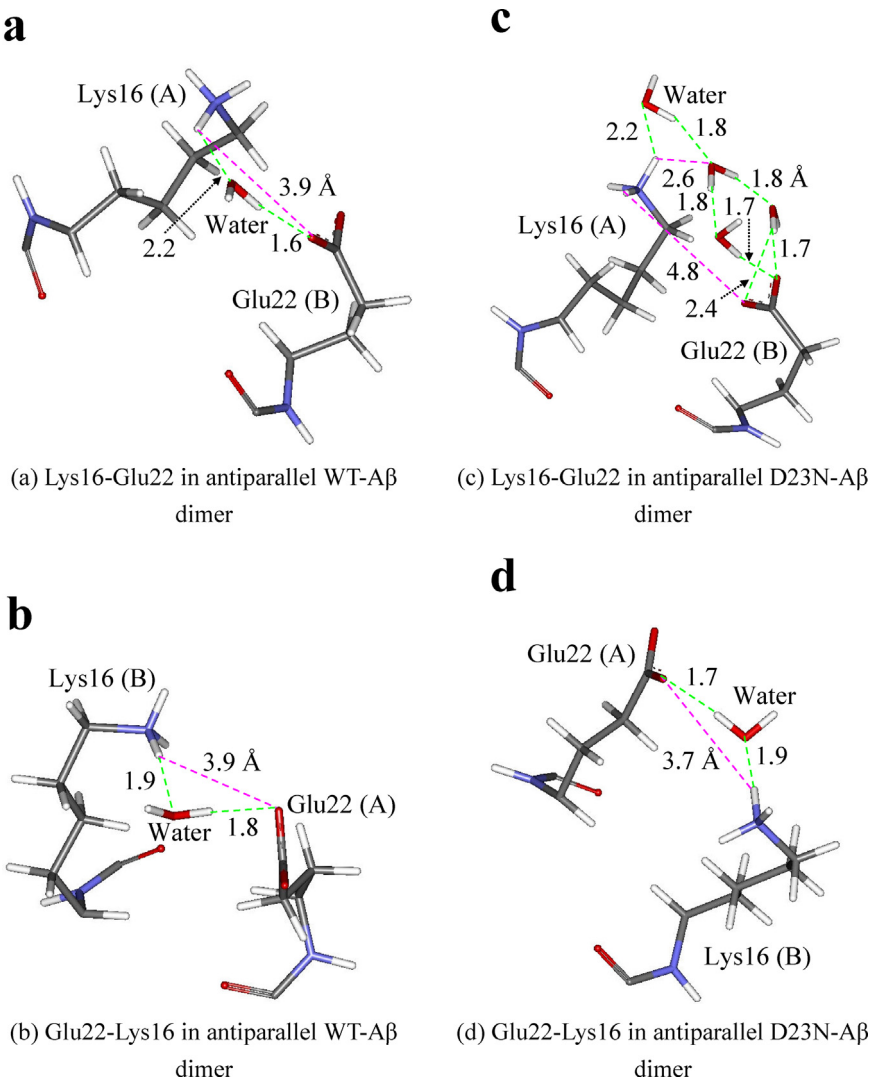

(a) Lys16-Glu22 in antiparallel WT-Aβ dimer

(c) Lys16-Glu22 in antiparallel D23N-Aβ dimer

(b) Glu22-Lys16 in antiparallel WT-Aβ dimer

(d) Glu22-Lys16 in antiparallel D23N-Aβ dimer

Fig. 5. Interacting structures between some amino acid residues of Monomer-A and B in the WT- and the D23N-Aβ(15–40) dimers with an antiparallel conformation; (a) and (c) between Lys16 of Monomer-A and Glu22 of Monomer-B, (b) and (d) between Glu22 of Monomer-A and Lys16 of Monomer-B. Green dash-lines indicate hydrogen bonds, while pink dash-lines indicate 5 electrostatic attractive interactions between charged amino acid residues. Some water molecules contribute to the interaction. (For interpretation of the references to color in figure legend, the reader is referred to the web version of the article.)

expected that this strong attractive interaction is the main cause for the stability of the parallel conformation of the WT-Aβ(15–40) dimer, in spite of the repulsive interactions of the Lys16–Lys16, Glu22–Glu22 and Lys28–Lys28 pairs.

In contrast, as indicated in Fig. 3b, the WT-Aβ(15–40) dimer with an antiparallel conformation has no strong repulsive interaction, because the above mentioned charged residues are separated to each other in the antiparallel conformation as shown in Fig. 1b. As a result, the BE between the WT-Aβ(15–40) monomers in the antiparallel conformation is significantly larger than that in the parallel conformation. Moreover, in the antiparallel conformation, there are strong attractive interactions; −97.8 kcal/mol between Lys16 and Glu22 and −62.3 kcal/mol between Glu22 and Lys16. As indicated in Fig. 5a and b, the shortest distance between Lys16 and Glu22 is 3.9 Å, and the direct salt bridge is not formed between these residues, being comparable to the result of the previous experiment [22]. Furthermore, Fig. 5a and b elucidates that a water molecule contributes to the attractive interaction between Glu22 and Lys16. The previous experimental study [21] proposed that the charged side chain of Lys28 has attractive interaction with the C-terminal charged carboxylate group of Val40. In the present study, however, since the C- and N- terminals of the Aβ monomers are terminated by the noncharged groups, the attractive interaction between Lys28 and Val40 is not observed.

We finally investigated the effect of the D23N mutation on the specific interaction between Aβ monomers. As shown in Fig. 4e–g, in the parallel D23N-Aβ(15–40) dimer, the distances for Lys16-Lys16, Glu22-Glu22 and Lys28-Lys28 pairs are 4.6, 3.8 and 5.5 Å, respectively. The distances for Lys16-Lys16 and Glu22-Glu22 are not affected by the D23N mutation significantly, while the distance of Lys28-Lys28 is elongated by 2.3 Å. This large change is related with the fact that the salt bridge between Asp23 and Lys28 is broken by the D23N mutation. As a result, the side chain of Lys28 becomes more flexible, and the two Lys28 are separated from each other in the parallel D23N-Aβ(15–40) dimer. On the other hand, in the antiparallel D23N-Aβ(15–40) dimer, as shown in Fig. 5c, there are many water molecules around the Lys16 and Glu22. As a result, the electrostatic attractive interaction between Lys16 and Glu22 is weakened by the solvating water molecules, leading the elongation of the distance between Lys16 and Glu22.

To elucidate the effect of the D23N mutation on the interactions between Aβ monomers, we analyzed the difference in IE map between the WT- and the D23N-Aβ(15–40) dimers. As shown in Fig. 3g and h, the electrostatic interactions

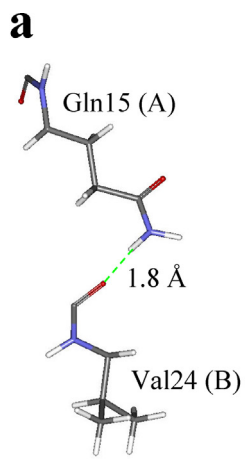

(a) Gln15-Val24 in antiparallel WT-Aβ dimer

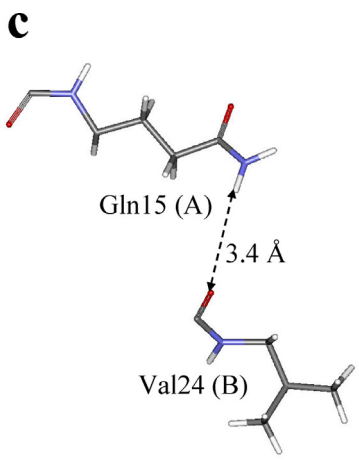

(c) Gln15-Val24 in antiparallel D23N-Aβ dimer

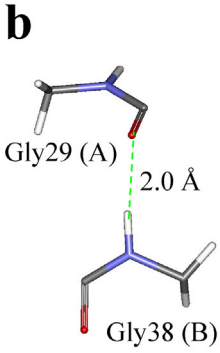

(b) Gly29-Gly38 in antiparallel WT-Aβ dimer

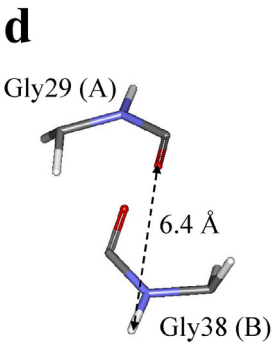

(d) Gly29-Gly38 in antiparallel D23N-Aβ dimer

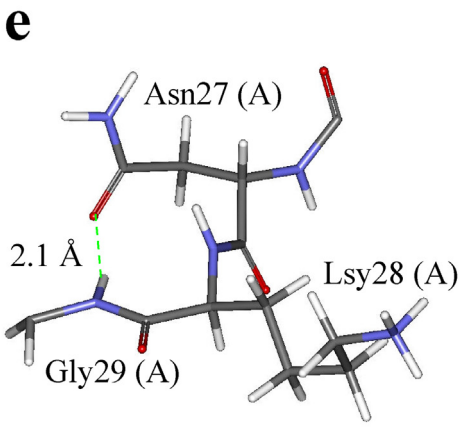

(e) Asn27-Gly29 in antiparallel D23N-Aβ dimer

Fig. 6. Interacting structures between some amino acid residues of Monomer-A and B in the WT- and the D23N-Aβ(15–40) dimers with an antiparallel conformation; (a) and (c) between Gln15 of Monomer-A and Val24 of Monomer-B, (b) and (d) between Gly29 of Monomer-A and Gly38 of Monomer-B, (e) between Asn27 and Gly29 of Monomer-A. Green dash-lines indicate hydrogen bonds. (For interpretation of the references to color in figure legend, the reader is referred to the web version of the article.)

involving Asp23 are significantly affected by the D23N mutation. As for the Aβ dimer with a parallel conformation, Fig. 3g indicates that the interaction between Asp23 of the monomer-A and Lys28 of the monomer-B is significantly weakened by the D23N mutation. In the WT-Aβ(15–40) dimer, Asp23 and Lys28 form a salt bridge as shown in Fig. 4d, and the interaction energy is–119.3 kcal/mol. Therefore, this large attractive interaction is a main source for the formation of the WT-Aβ dimer.

In contrast, as shown in Fig. 4h, in the parallel D23N-Aβ(15–40) dimer, Asn23 and Lys28 are separated from each other, resulting in the weak interactions between the D23N-Aβ monomers. Therefore, it is expected that the parallel conformation of the D23N-Aβ

monomers is less stable than that of the WT-Aβ monomers. In the previous studies [25,26,44], it was suggested that the salt bridge between Glu22/Asp23 and Lys28 is a driving force for the oligomerization and the fibrillation of Aβ monomers. The present simulations elucidate that the D23N mutation causes the destabilization of attractive electrostatic interactions between Asn23 and Lys28 of the different monomers.

To elucidate the effect of the D23N mutation on the Aβ(15–40) dimer with an antiparallel conformation, we investigated the difference in the IE map between the antiparallel WT- and D23N-Aβ dimers. As shown in Fig. 3h, the effect is much smaller compared with that (Fig. 3g) for the parallel conformation. The interaction energies for the Gln15(A)–Val24(B), Lys16(A)–Glu22(B) and Gly29(A)–Gly38(B) pairs are reduced by 10 kcal/mol. In order to clarify the reason for these changes, we looked into the structures around the residues. As shown in Fig. 6a, in the antiparallel WT-Aβ(15–40) dimer, the side chain of Gln15 and the backbone oxygen of Val24 are hydrogen bonded. In contrast, in the antiparallel D23N-Aβ(15–40) dimer, Gln15 and Val24(B) are separated from each other, as shown in Fig. 6c. In the similar way, Gly29 and Gly38 are hydrogen bonded in the antiparallel WT-Aβ(15–40) dimer as shown Fig. 6b, while these residues are separated in the D23N-Aβ dimer (Fig. 6d). As for the interaction between Lys16 and Glu22, as mentioned before, the distance between them is changed by the effect of solvating water molecules, resulting in the change in interaction energy.

The optimized structures of the solvated Aβ(15–40) dimer and the specific interactions between the monomers clarify that the effects of D23N mutation on the dimer structure are significant for the parallel conformation, while the effect is smaller for the antiparallel conformation. Comparison of the interaction energies between monomers for the WT- and the D23N-Aβ(15–40) dimers indicates that the D23N mutation causes destabilization of electrostatic interactions between Aβ monomers. Moreover, the effect of solvating water molecules on the dimer structure is revealed at an electronic level; (1) solvating water molecules have a significant affect on the relative stability of the Aβ dimer conformation, (2) they also involve in the specific inter-monomer interaction between Lys16 and Glu22 in the antiparallel Aβ conformation.

4. Conclusions

We here investigated stable structures for the solvated WT-Aβ(15–40) dimer and the D23N mutated-Aβ(15–40) dimer depending on their conformations, using classical MM method, with solvating water molecules considered explicitly. In addition, the specific interactions between the Aβ residues and the water molecules and between the Aβ residues of the different monomers were elucidated by the *ab initio* FMO calculations. The results are summarized as follows.

(1) In water, the parallel conformation is more stable than the antiparallel one, due to the larger hydration energy for the parallel conformation for both the WT- and the D23N- Aβ(15–40) dimers.
(2) In the parallel conformation of the WT-dimer, the salt-bridge between Asp23 and Lys28 and the electrostatic interactions between the charged residues of Aβ and the solvating water molecules contribute mainly to the dimer stability.
(3) By the D23N mutation, the salt-bridge between Asp23 and Lys28 in the parallel conformation is disappeared, resulting in a reduction of the stability for the parallel conformation of Aβ dimer.

Acknowledgements

This work was supported in part by the grants from the Murata Science Foundation and the Hori Science and Arts Foundation.

References

[1] F.M. Laird, H. Cai, A.V. Savonenko, M.H. Farah, K. He, T. Melnikova, T. Wen, H.-C. Chiang, G. Xu, V.E. Koliatsos, D.R. Borchelt, D.L. Price, H.-K. Lee, H.-K. Wong, BACE1, a major determinant of selective vulnerability of the brain to amyloid-β amyloidogenesis, is essential for cognitive, emotional, and synaptic functions, J. Neurosci. 25 (2005) 11693–11709.
[2] D.J. Selkoe, Alzheimer's disease: genes, proteins, and therapy, Physiol. Rev. 81 (2001) 741–766.
[3] M. Rak, M.R.D. Bigio, S. Mai, D. Westaway, K. Gough, Dense-core and diffuse Aβ plaques in TgCRND8 mice studied with synchrotron FTIR microspectroscopy, Biopolymers 87 (2007) 207–217.
[4] S.A. Gravina, L. Ho, C.B. Eckman, K.E. Long, L. Otvos Jr., L.H. Younkin, N. Suzuki, S.G. Younkin, Amyloid-β protein (Aβ) in Alzheimer's disease brain, J. Biol. Chem. 270 (1995) 7013–7016.
[5] A.E. Roher, J.D. Lowenson, S. Clarke, A.S. Woods, R.J. Cotter, E. Gowing, M.J. Ball, β-Amyloid-(1–42) is a major component of cerebrovascular amyloid deposits: implications for the pathology of Alzheimer disease, Proc. Natl. Acad. Sci. U.S.A. 90 (1993) 10836–10840.
[6] J.T. Jarrett, E.P. Berger, P.T. Lansbury Jr., The carboxy terminus of the β-amyloid protein is critical for the seeding of amyloid formation: implications for the pathogenesis of Alzheimer's disease, Biochemistry 32 (1993) 4693–4697.
[7] M.A. Findeis, The role of amyloid β peptide 42 in Alzheimer's disease, Pharmacol. Ther. 116 (2007) 266–286.
[8] S.W. Pimplikar, Reassessing the amyloid cascade hypothesis of Alzheimer's disease, Int. J. Biochem. Cell Biol. 41 (2008) 1261–1268.
[9] R. Tycko, Characterization of amyloid structures at the molecular level by solid state nuclear magnetic resonance spectroscopy, Methods Enzymol. 413 (2006) 103–122.
[10] R. Tycko, Molecular structure of amyloid fibrils: insights from solid state NMR, Q. Rev. Biophys. 39 (2006) 1–55.
[11] J.J. Balbach, A.T. Petkova, N.A. Oyler, O.N. Antzutkin, D.J. Gordon, S.C. Meredith, R. Tycko, Supramolecular structure in full-length Alzheimer's β-amyloid fibrils: evidence for a parallel betasheet organization from solid-state nuclear magnetic resonance, Biophys. J. 83 (2002) 1205–1216.
[12] T.L. Benzinger, D.M. Gregory, T.S. Burkoth, H. Miller-Auer, D.G. Lynn, R.E. Botto, S.C. Meredith, Propagating structure of Alzheimer's β-amyloid(10–35) is parallel β-sheet with residues in exact register, Proc. Natl. Acad. Sci. U.S.A. 95 (1998) 13407–13412.
[13] O.N. Antzutkin, J.J. Balbach, R.D. Leapman, N.W. Rizzo, J. Reed, R. Tycko, Multiple quantum solid-state NMR indicates a parallel, not antiparallel, organization of β-sheets in Alzheimer's β-amyloid fibrils, Proc. Natl. Acad. Sci. U.S.A. 97 (2000) 13045–13050.
[14] A.T. Petkova, R.D. Leapman, Z.H. Guo, W.M. Yau, M.P. Mattson, R. Tycko, Self-propagating, molecularlevel polymorphism in Alzheimer's β-amyloid fibrils, Science 307 (2005) 262–265.
[15] A.K. Paravastu, R.D. Leapman, W.M. Yau, R. Tycko, Molecular structural basis for polymorphism in Alzheimer's β-amyloid fibrils, Proc. Natl. Acad. Sci. U.S.A. 105 (2008) 18349–18354.
[16] J.C. Chan, N.A. Oyler, W.M. Yau, R. Tycko, Parallel, β-sheets and polar zippers in amyloid fibrils formed by residues 10–39 of the yeast prion protein Ure2p, Biochemistry 44 (2005) 10669–10680.
[17] F. Shewmaker, R.B. Wickner, R. Tycko, Amyloid of the prion domain of Sup35p has an in-register parallel β-sheet structure, Proc. Natl. Acad. Sci. U.S.A. 103 (2006) 19754–19759.
[18] M. Török, S. Milton, R. Kayed, P. Wu, T. McIntire, C.G. Glabe, R. Langen, Structural and dynamic features of Alzheimer's Aβ peptide in amyloid fibrils studied by site-directed spin labeling, J. Biol. Chem. 277 (2002) 40805–40810.
[19] A. Der-Sarkissian, C.C. Jao, J. Chen, R. Langen, Structural organization of alpha-synuclein fibrils studied by site-directed spin labeling, J. Biol. Chem. 278 (2003) 37530–37535.
[20] S. Luca, W.M. Yau, R. Leapman, R. Tycko, Peptide conformation and supramolecular organization in amylin fibrils: constraints from solid-state NMR, Biochemistry 46 (2007) 13505–13522.
[21] R. Tycko, K.L. Sciarretta, J. Orgel, S.C. Meredith, Evidence for novel β-sheet structures in Iowa mutant β-amyloid fibrils, Biochemistry 48 (2009) 6072–6084.
[22] W. Qiang, W.M. Yau, Y. Luo, M.P. Mattson, R. Tycko, Antiparallel β-sheet architecture in Iowa-mutant β-amyloid fibrils, Proc. Natl. Acad. Sci. U.S.A. 109 (2012) 4443–4448.
[23] T.J. Grabowski, H.S. Cho, J.P.G. Vonsattel, G.W. Rebeck, S.M. Greenberg, Novel amyloid precursor protein mutation in an Iowa family with dementia and severe cerebral amyloid angiopathy, Ann. Neurol. 49 (2001) 697–705.
[24] W. van Nostrand, J.P. Melchor, H.S. Cho, S.M. Greenberg, G.W. Rebeck, Pathogenic effects of D23N Iowa mutant amyloid β-protein, J. Biol. Chem. 276 (2001) 32860–32866.
[25] T. Lührs, C. Ritter, M. Adrian, D. Riek-Loher, B. Bohrmann, H. Döbeli, D. Schubert, R. Riek, 3D structure of Alzheimer's amyloid-β(1–42) fibrils, Proc. Natl. Acad. Sci. U.S.A. 102 (2005) 17342–17347.

[26] A.T. Petkova, W.-M. Yau, R. Tycko, Experimental constraints on quaternary structure in Alzheimer's β-amyloid fibrils, Biochemistry 45 (2006) 498–512.
[27] D. Fedorov, K. Kitaura, Extending the power of quantum chemistry to large systems with the fragment molecular orbital method, J. Phys. Chem. A 111 (2007) 6904–6914.
[28] K. Kitaura, E. Ikeo, T. Asada, T. Nakano, M. Uebayasi, Fragment molecular orbital method: an approximate computational method for large molecules, Chem. Phys. Lett. 313 (1999) 701–706.
[29] K. Kitaura, T. Sawai, T. Asada, T. Nakano, M. Uebayasi, Pair interaction molecular orbital method: an approximate computational method for molecular interactions, Chem. Phys. Lett. 312 (1999) 319–324.
[30] T. Nakano, T. Kaminuma, T. Sato, Y. Akiyama, M. Uebayasi, K. Kitaura, Fragment molecular orbital method: application to polypeptides, Chem. Phys. Lett. 318 (2000) 614–618.
[31] T. Nakano, T. Kaminuma, T. Sato, K. Fukuzawa, Y. Akiyama, M. Uebayasi, K. Kitaura, Fragment molecular orbital method: use of approximate electrostatic potential, Chem. Phys. Lett. 351 (2002) 475–480.
[32] K. Kitaura, S. Sugiki, T. Nakano, Y. Komeiji, M. Uebayasi, Fragment molecular orbital method: analytical energy gradients, Chem. Phys. Lett. 336 (2001) 163–170.
[33] M. Ito, K. Fukuzawa, T. Ishikawa, Y. Mochizuki, T. Nakano, S. Tanaka, Ab initio fragment molecular orbital study of molecular interactions in liganded retinoid X receptor: specification of residues associated with ligand inducible information transmission, J. Phys. Chem. B 112 (2008) 12081–12094.
[34] Y. Mochizuki, K. Yamashita, T. Murase, T. Nakano, K. Fukuzawa, K. Takematsu, H. Watanabe, S. Tanaka, Large scale FMO-MP2 calculations on a massively parallel-vector computer, Chem. Phys. Lett. 457 (2008) 396–403.
[35] D.G. Fedorov, T. Nagata, K. Kitaura, Exploring chemistry with the fragment molecular orbital method, Phys. Chem. Chem. Phys. 14 (2012) 7562–7577.
[36] K. Arnold, L. Bordoli, J. Kopp, T. Schwede, The SWISS-MODEL workspace: a web-based environment for protein structure homology modelling, Bioinformatics 22 (2006) 195–201.
[37] D. Van Der Spoel, E. Lindahl, B. Hess, G. Groenhof, A.E. Mark, H.J. Berendsen, GROMACS: fast, flexible, and free, J. Comput. Chem. 26 (2005) 1701–1718.
[38] V. Hornak, R. Abel, A. Okur, B. Strockbine, A. Roitberg, C. Simmerling, Comparison of multiple Amber force fields and development of improved protein backbone parameters, Proteins 65 (2006) 712–725.
[39] H.W. Horn, W.C. Swope, J.W. Pitera, J.D. Madura, T.J. Dick, G.L. Hura, T. Head-Gordon, Development of an improved four-site water model for biomolecular simulations: TIP4P-Ew, J. Chem. Phys. 120 (2004) 9665–9678.
[40] N.L. Fawzi, A.H. Phillips, J.Z. Ruscio, M. Doucleff, D.E. Wemmer, T. Head-Gordon, Structure and dynamics of the Aβ(21–30) peptide from the interplay of NMR experiments and molecular simulations, J. Am. Chem. Soc. 130 (2008) 6145–6158.
[41] Y. Mochizuki, K. Yamashita, T. Nakano, Y. Okiyama, K. Fukuzawa, N. Taguchi, S. Tanaka, Higher-order correlated calculations based on fragment molecular orbital scheme, Theor. Chem. Acc. 130 (2011) 515–530.
[42] A.T. Petkova, Y. Ishii, J.J. Balbach, O.N. Antzutkin, R.D. Leapman, F. Delaglio, R. Tycko, A structural model for Alzheimer's β-amyloid fibrils based on experimental constraints from solid state NMR, Proc. Natl. Acad. Sci. U.S.A. 99 (2002) 16742–16747.
[43] N.V. Buchete, G. Hummer, Structure, Dynamics of parallel β-sheets, hydrophobic core, and loops in Alzheimer's Aβ fibrils, Biophys. J. 92 (2007) 3032–3039.
[44] P. Anand, F.S. Nandel, U.H. Hansmann, The Alzheimer, β-amyloid ($A\beta_{1-39}$) dimer in an implicit solvent, J. Chem. Phys. 129 (2008) 195102.
[45] K. Fukuzawa, T. Nakano, A. Kato, Y. Mochizuki, S. Tanaka, Applications of the fragment molecular orbital method for bio-macromolecules, J. Comput. Chem. 6 (2007) 185–198.